Ground States and Phase Ordering Studies of the Random Field Ising Model

Varsha Banerjee

Department of Physics
IIT Delhi

December 29, 2017

Outline

I. Random Field Ising Model (RFIM)

II. Ground States ($T = 0$)

- Graph-Cut Method
- Determination of Critical Points
- Textures of Domains and Interfaces

III. Phase Ordering after a Thermal Quench ($T \neq 0$)

- Dynamical Scaling and Super-Universality Violations
- Algebraic vs. Logarithmic Growth Laws

IV. Summary

Collaborators - Gaurav Shrivastav, Manoj Kumar, Arunkumar Bupathy, Sanjay Puri (JNU)

I. Random Field Ising Model

The Random Field Ising Model (RFIM) is an archetypal example of a system with disorder and frustration.

- Energy function

$$E = -J \sum_{\langle ij \rangle} s_i s_j - \sum_{i=1}^{N} h_i s_i, \quad s_i = \pm 1.$$

  - The interaction $J > 0$ prefers a magnetized structure.
  - The disordering random fields $\{h_i\}$ are generally drawn from:

$$P(h_i) = \frac{1}{\sqrt{2\pi}\Delta} e^{(-h_i{}^2/2\Delta^2)}.$$

  - Small region of (T, Δ)-values where equilibrium phase is ferromagnetic $(d = 3)$. $T_c(\Delta = 0) \simeq 4.51$, $\Delta_c(T = 0) \simeq 2.28$.

Some Experimental Realizations of the RFIM

- Diluted antiferromagnets (DAFs) in a uniform field.

  Fishman & Aharony, J. Phys. C, 1978; Ye et al, PRB 2006; Miga et al., PRB, 2009

- Dipolar quantum magnet $LiHo_xY_{1-x}F_4$.

  Schechter & Stamp, PRL, 2005; Schechter, PRB, 2008

- Binary mixture (AB) in porous medium (oil-water, colloid-polymer).

  P.G. De Gennes, J. Phys. Chem. Lett., 1984; Vink et al.,PRL, 2006

Ising spins do not have an intrinsic dynamics. Contact with heat bath generates stochastic spin-flips.

- Glauber model with non-conserved kinetics. (DAFFs, $LiHo_xY_{1-x}F_4$.)
- Kawasaki model with conserved kinetics. (Binary mixture with A $\leftrightarrow$ B interchanges.)
- Although the two models describe different time-dependent behavior, the equilibrium state is unique.

Difficulties with Disorder

- Competing interactions create a complex free energy landscape:

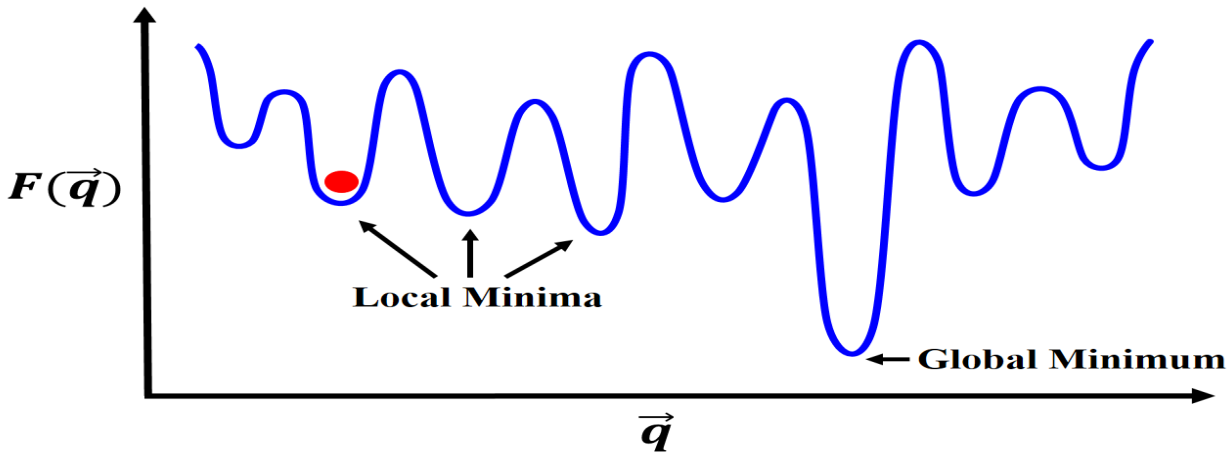

- Many local minima separated by energy barriers $\sim O(e^N)$.
- Standard minimisation procedures such as Metropolis, Cluster, Parallel Tempering, etc. involve $O(1)$ spin-flips at a time; Convergence time to global minimum is non-polynomial in N.
- System opts for a local minimum far from the global minimum.

II. Max-Flow/Min-Cut or Graph Cut Methods

A specialized graph for the energy function is constructed such that the cheapest cut on the graph minimizes energy either globally or locally.

- The cut enables simultaneous relabeling of several spins or nodes.
- Large portion of the phase-space can be sampled in one move.
- The convergence time to the global minimum is polynomial in N.
  - Ford-Fulkerson - $O(N^3)$ *Flows in Networks*, **Princeton University Press, 1962**
  - Goldberg-Tarjan - $O(N^3)$ **J. ACM, 1988**
  - Boykov-Kolmogorov - $O(N)$ **IEEE Transactions on PAMI, 2004**
- Facilitate search for a "good quality" local minimum, if the global minimum is difficult to reach.
- Often provide optimality bounds.

Background on Graphs

- A graph $\mathcal{G} = (\mathcal{V}, \mathcal{E})$ consisting of vertices $\mathcal{V}$ and edges $\mathcal{E}$ that connect then.
- An edge ij joining vertices i and j is assigned a weight V_{ij}.
- A cut C is a partition of the vertices $\mathcal{V}$ into two sets $\mathcal{R}$ and $\mathcal{Q}$.
- Any edge $ij \in \mathcal{E}$ with $i \in \mathcal{R}$ and $j \in \mathcal{Q}$ (or vice-versa) is a cut edge.
- The cost of the cut is defined to be the sum of the weights of the edges crossing the cut.
- The min-cut problem is to find the cut with the smallest cost.

The Graph Construction

- A standard energy function:

$$E(\{s_i\}) = \sum_{\{ij\}\in\mathcal{N}} V_{ij}(s_i, s_j) + \sum_i D_i(s_i), \quad s_i \in \mathcal{L} = (\alpha, \beta, ..., \gamma),$$
$$= E_{smooth} + E_{data}.$$

- Two-terminal graph ($s_i = \alpha, \beta$):

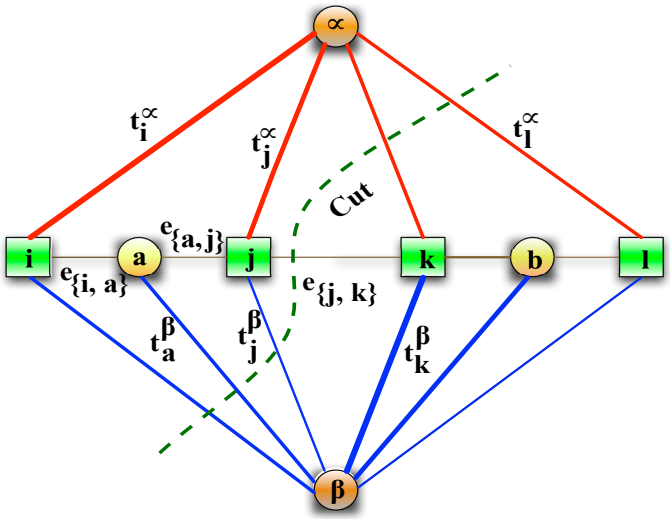

(Boykov & Kolmogorov , IEEE PAMI, 2004)

Edge	Weight	For
t_i^{β}	∞	$i \in \mathcal{R}_{\alpha}$
t_i^{β}	$D_i(s_i)$	$i \notin \mathcal{R}_{\alpha}$
t_i^{α}	$D_i(\alpha)$	$i \in \mathcal{R}_{\alpha}$
$e_{\{i,a\}}$	$V(s_i, \alpha)$	$\{i,j\} \in \mathcal{N}, s_i \neq s_j$
$e_{\{a,j\}}$	$V(\alpha, s_j)$	
t_a^{β}	$V(s_i, s_j)$	
$e_{\{i,j\}}$	$V(s_i, \alpha)$	$\{i,j\} \in \mathcal{N}, s_i = s_j$

When can the Global Minimum be reached?

- Exact min-cut can be found in polynomial time if
  1. E is quadratic,
  2. s_i's are binary (0 or 1 say),
  3. interactions satisfy the regularity condition:

$$V_{ij}(0,0) + V_{ij}(1,1) \leq V_{ij}(1,0) + V_{ij}(0,1).$$

(Picard, Ratliff, Networks, 1975; Papadimitriou, Steiglitz, Combinatorial Optimization, 1982)

- $n_i = (1 + \sigma_i)/2$ transforms $\sigma_i = \pm 1$ to $n_i = 0, 1$.
- In physical systems, 3 corresponds to interactions $J_{ij} > 0$.
- Ground states of the RFIM are assured by min-cut algorithms.

(d'Auriac, Preissmann, Rammal, J. Phys. (France) Lett. 1985)

Comparison between MC and BK-GCM

- Morphologies for a lattice of size 128^3 and disorder $\Delta = 2.4$:

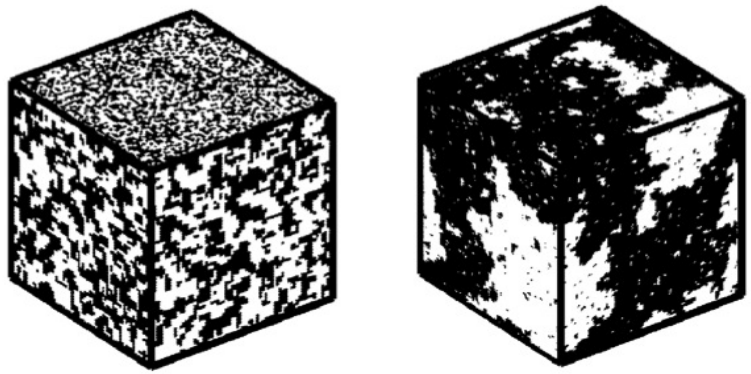

(a) Steady-state morphology using the MC method;
(b) Ground-state morphology obtained using the BK-GCM.

- MC morphology is not as compact or well defined.
- Energy per spin: $\simeq$ -3.05 (BK-GCM); $\simeq$ -2.69 (MC).
- The BK-GCM yields a 99% overlap with the GS in the first iteration.

Δ_c of isometric lattices

Binder cumulant $U_4 = 1 - \langle m^4 \rangle / 3 \langle m^2 \rangle^2, \quad m = N^{-1} \sum_{i=1}^{N} s_i$

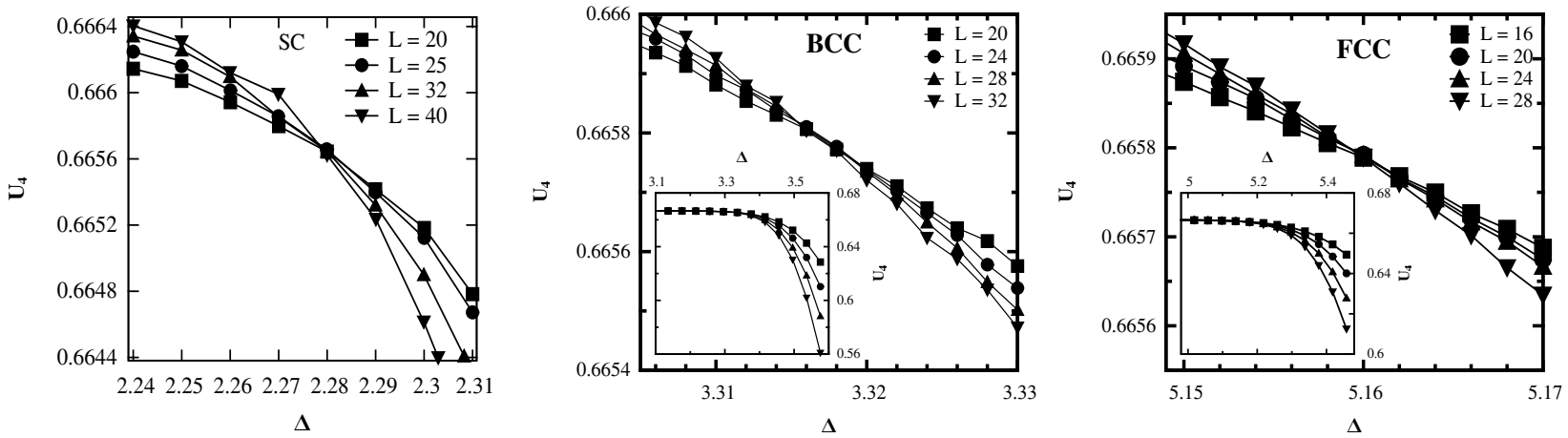

	SC (6)	BCC (8)	FCC (12)
Δ_c	2.278 ± 0.002	3.316 ± 0.002	5.160 ± 0.002

Averaging over $\sim 10^6$ disorder realizations; Symbols size $\equiv$ error bar.

(Shrivastav, Kumar, VB, Puri, Phys. Rev. E, 2014)

(Bupathy, VB, Puri, Phys. Rev. E, 2016)

Ground State Morphologies

(Bupathy, VB, Puri, Phys. Rev. E, 2016)

$L = 160$; $\delta = (\Delta - \Delta_c)/\Delta_c$; SC: L^3, BCC: $2 \times L^3$, FCC: $4 \times L^3$.

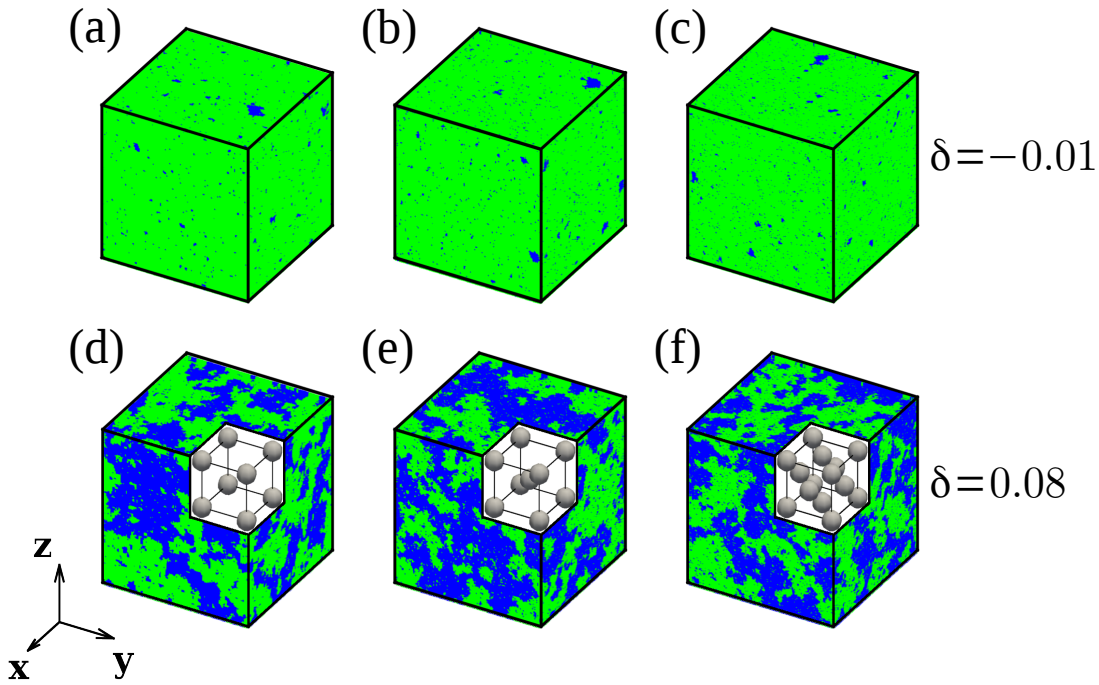

- The green and blue regions correspond to $s_i = 1$ and $s_i = -1$.
- Emergence of domains of size ξ as Δ reduced from $\Delta = \infty$.
- $\xi \to \infty$ as $\Delta \to \Delta_c^+$.

Tools for Characterizing GS Morphologies

- Standard probe is the correlation function:

$$C(r) \quad = \quad \langle \psi(\vec{r_i})\, \psi(\vec{r_j}) \rangle - \langle \psi(\vec{r_i}) \rangle \langle \psi(\vec{r_j}) \rangle,$$

where $\psi(\vec{r_i})$ is an appropriate variable [s_i] and $r = |\overrightarrow{r_i} - \overrightarrow{r_j}|$. The angular brackets denote an ensemble average.

Correlation length ξ: Distance over which $C(r)$ decays to (say) $0.2\times$ maximum value.

- Small-angle scattering experiments yield the structure factor:

$$S(\vec{k}) = \int d\vec{r} e^{i\vec{k}\cdot\vec{r}} C(r),$$

where $\vec{k}$ is the wave-vector of the scattered beam.

Rough Interfaces, Cusp Singularities and Non-Porod Tails

Interfaces separating correlated regions of up and down spins are rough in disordered systems with important implications in systemic relaxation.

- Small-r behavior exhibits a *cusp singularity*:

$$C(r,t;\Delta) = 1 - Ax^{\alpha} + O(x^{2+\alpha}),$$

  where $x = r/\xi$, A is a constant, and α is the *cusp exponent.*

- For smooth interfaces, $\alpha = 1$. For fractal interfaces, $0 < \alpha < 1$ and the fractal dimension $d_f = d - \alpha$. (d is the Euclidian dimension.)

- For $\alpha = 1$, $S(k,\Delta) \sim k^{-(d+1)}$ yielding the Porod law due to scattering from smooth interfaces.

- For $0 < \alpha < 1$, $S(k,\Delta) \simeq \tilde{A}(k\xi)^{-(d+\alpha)}$ exhibiting a non-Porod tail indicative of scattering off rough interfaces:

Europhys. Lett. 2013; Phys. Rev. E, 2014; Phys. Rev. E, 2016

Interfacial Features (Para Phase) (Bupathy, VB, Puri, Phys. Rev. E, 2016)

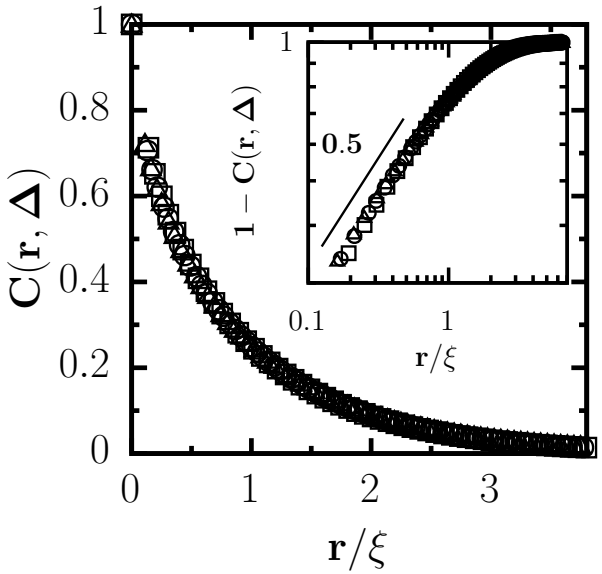

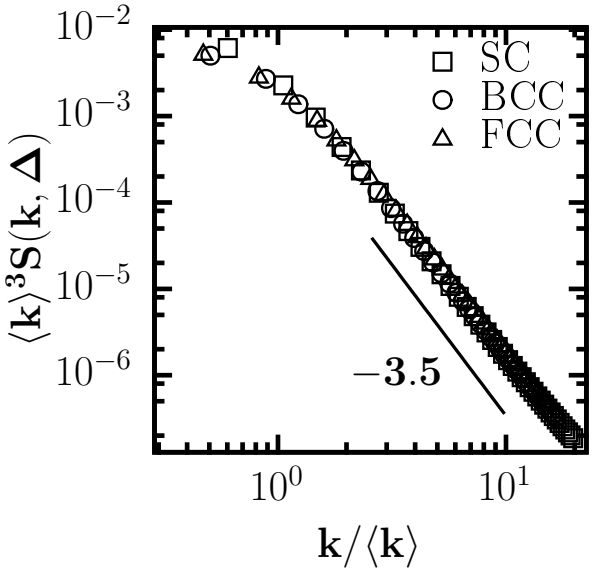

SC

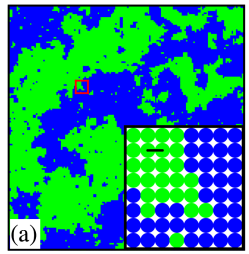

BCC

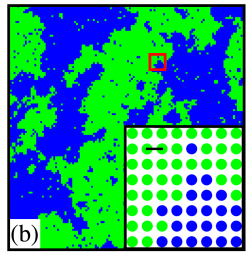

FCC

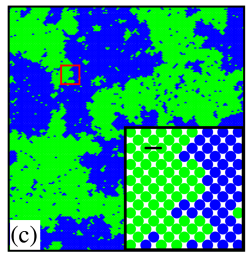

- *Universal* scaling function for all disorder amplitudes, disorder types and lattice types. The morphologies are characterized by a unique length scale $\xi(\Delta)$.

  (Kumar, VB, Puri, EPJE, 2017)

- Small-r behaviour characterized by a *universal* cusp exponent $\alpha \simeq 0.5$ with $d_f = 2.5$.

- Large-k behaviour exhibits *non-Porod tail* due to scattering off fractal interfaces.

Interfacial Features (Ferro Phase)

(Bupathy, VB, Puri, Phys. Rev. E, 2016)

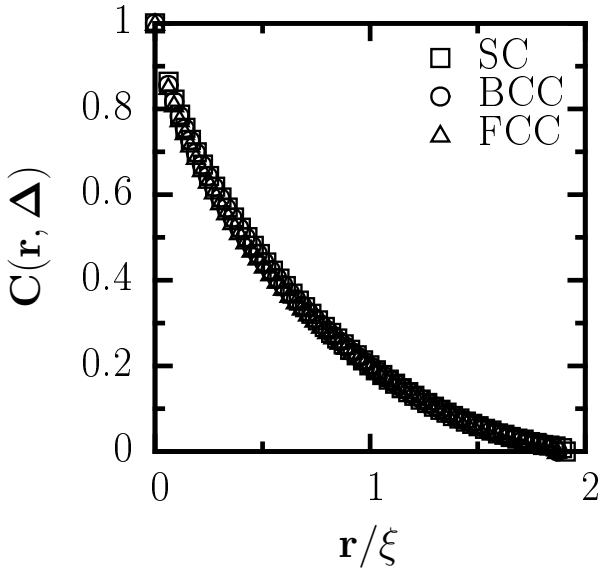

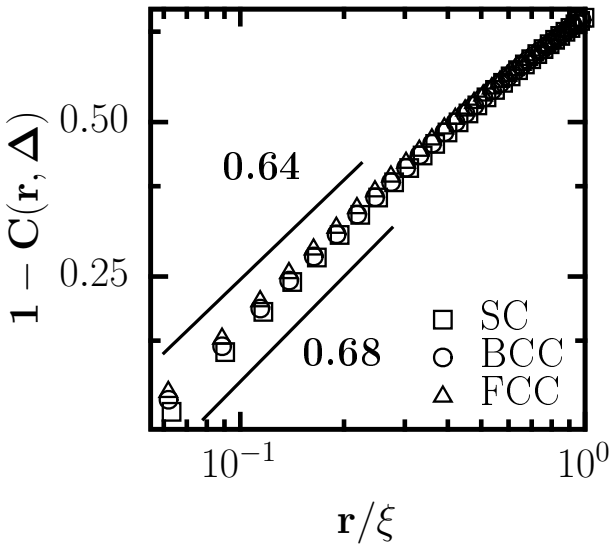

SC

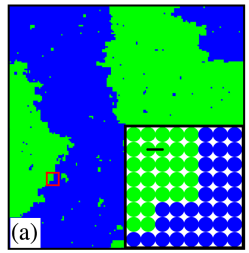

BCC

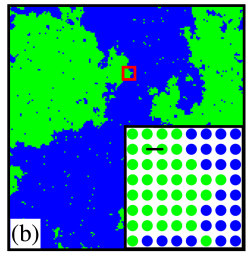

FCC

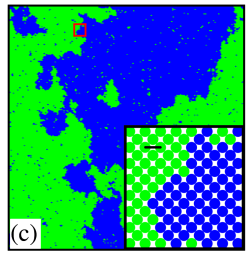

- Distinct cusp exponents from the para phase.
- $\alpha = 0.68 \pm 0.01$ (SC), 0.66 ± 1 (BCC) and 0.64 ± 1 (FCC).
- Though minor, these variations have important consequences for relaxation behaviour.

Comparisons with Experimental Data

- Small-angle scattering data from DAFs (para regime).

  (Belanger, *et al.*, Phys. Rev. B, 1985)

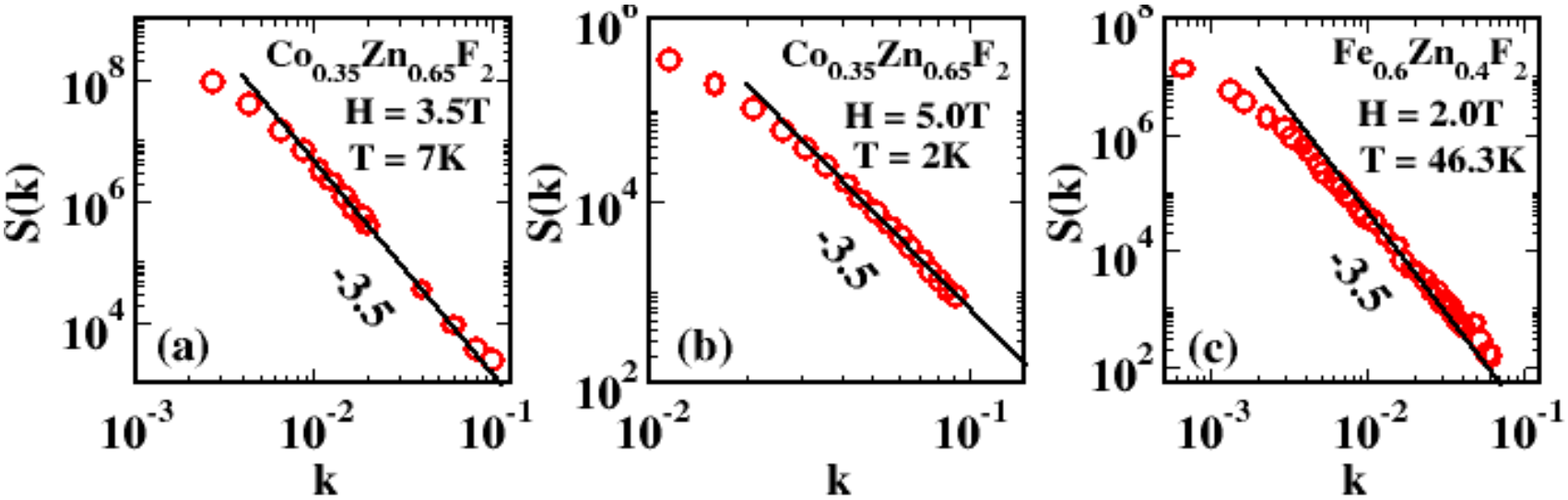

- All three data exhibit an asymptotic cusp regime $[S(k) \sim k^{-3.5}]$.

(Shrivastav, Kumar, VB, Puri, Phys. Rev. E, 2014)

III. Domain Growth after a Temperature Quench

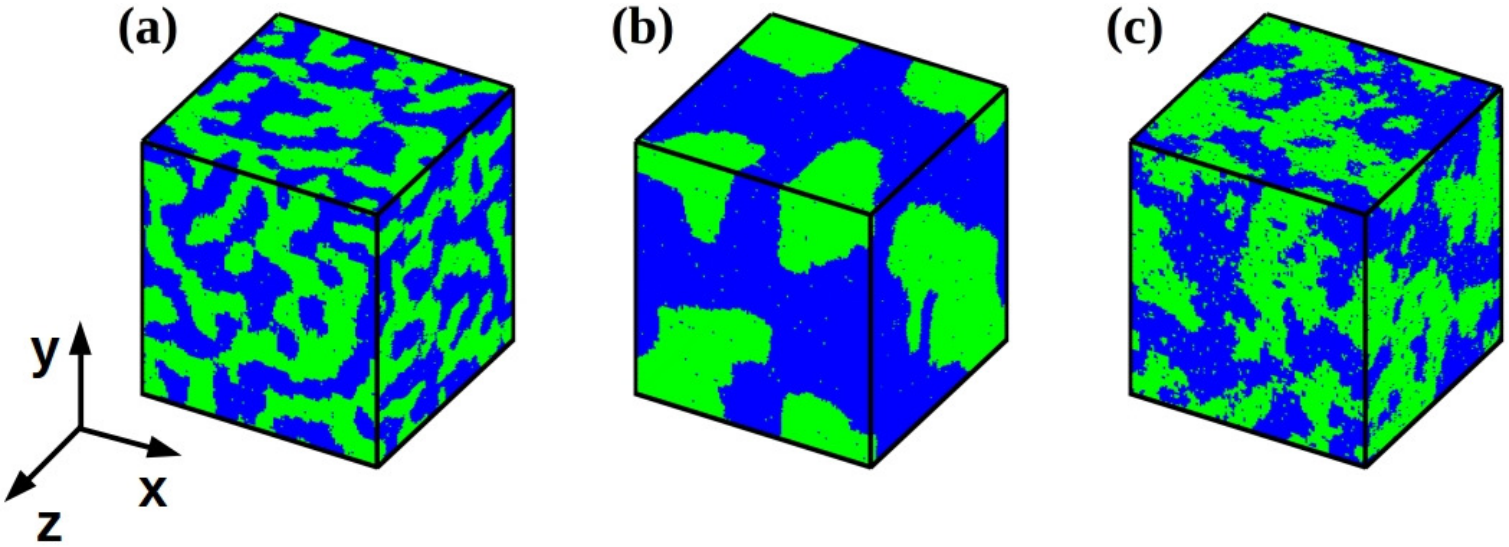

- Domain growth in $d = 3$ C-RFIM for (a) $\Delta = 1.0,\ t = 10^5$ MCS; (b) $\Delta = 1.0,\ t = 10^7$ MCS; and (c) $\Delta = 2.0,\ t = 10^7$ MCS.
- The lattice size is 128^3 and the temperature $T = 2 < T_c(\Delta)$.

Kumar, VB, Puri, Europhys. Lett. 2017

Interfacial Characteristics during Domain Growth

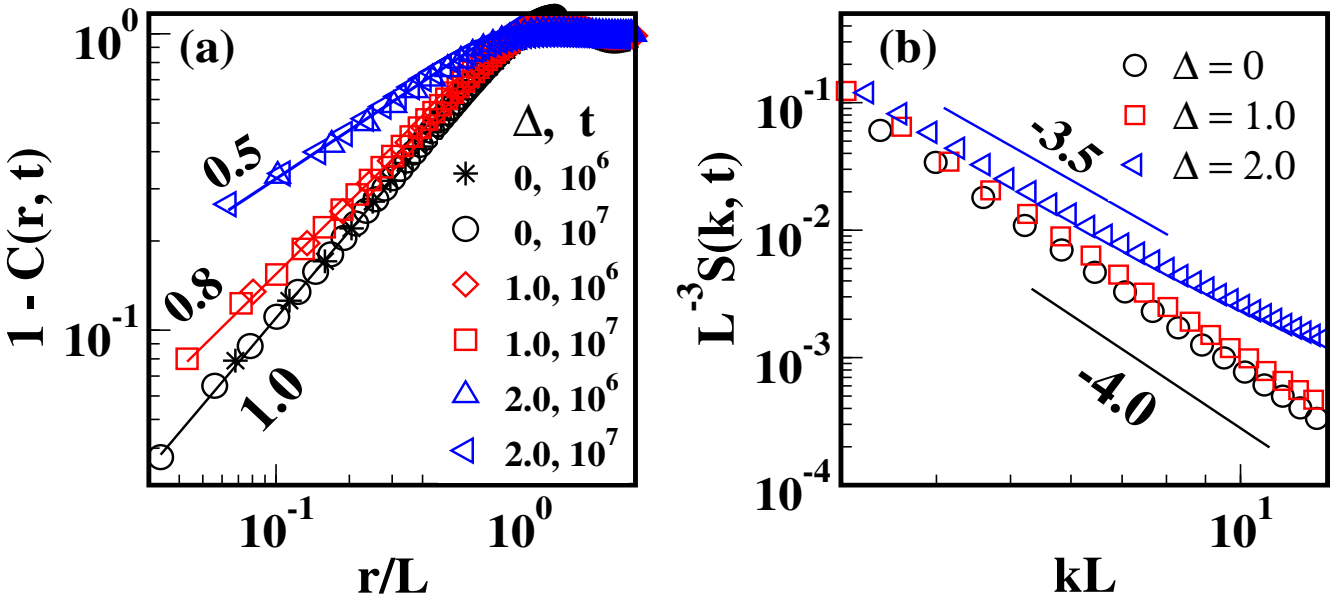

(a) Disorder-dependent roughness exponent $\alpha(\Delta) \simeq 1.0, 0.8, 0.5$ for $\Delta = 0, 1.0, 2.0$, respectively.

(b) Plot of scaled structure factor, $L(t)^{-d} S(k, t; \Delta)$ vs. $kL(t)$, for $t = 10^7$ MCS and $\Delta = 0, 1.0, 2.0$. Solid lines denote relevant Porod and non-Porod tails.

Kumar, VB, Puri, Europhys. Lett. 2017

Growth Laws: Algerbraic vs. Logarithmic

- Plot of the characteristic length scale, $L(t)$ vs. t on a log-log scale:

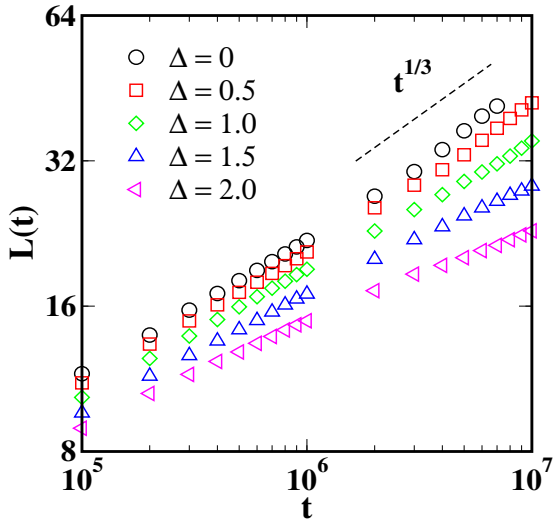

For pure systems ($\Delta = 0$):
$L(t) \sim t^{1/3}$.
Lifshitz-Slyozov (LS) law

- Notice the slowing down of domain growth at late times for higher disorder strengths.

(i) Algebraic growth at early times: $L(t, \Delta) \sim t^{1/\bar{z}}$ with disorder-dependent exponent $\bar{z}(\Delta)$. (For $\Delta = 0$, $\bar{z} = 3$.)

(ii) Cross-over to logarithmic domain growth at late times: $L(t, \Delta) \sim (\ln t)^{1/\psi}$, ψ is a disorder-independent *barrier* exponent.

Kumar, VB, Puri, Europhys. Lett. 2017

Scaling Ansatz to determine $\bar{z}$ and ψ

- Assume that the growth law scales as:

$$L(t, \Delta) \sim t^{1/z_{\text{eff}}} = t^{1/z} F(\Delta / t^{\phi}), \tag{1}$$

$$F(x) \sim \begin{cases} \text{const.}, & \text{for } x \to 0, \\ x^{1/\phi z}\, \ell\left(x^{-1/\phi}\right), & \text{for } x \to \infty. \end{cases} \tag{2}$$

z_{eff} is the *effective* growth exponent, ϕ is the *crossover* exponent.

Corberi et al. Phys. Rev. E 2012, 2013

- Cross-over from power law $L(t) \sim t^{1/z}$ to asymptotic form $L(t) \sim \ell\left(x^{-1/\phi}\right)$ if $\phi < 0$ and vice versa if $\phi > 0$.

- Disorder is asymptotically relevant if $\phi < 0$ and irrelevant if $\phi > 0$.

Exponents from Scaling of $L(t)$

- Parameters $\overline{z}$ and λ for different Δ-values.

$d = 2$	Δ	0	0.25	0.50	0.75	1.00
	$\overline{z}$	3.0	3.38	3.84	4.38	4.59
$d = 3$	Δ	0	0.5	1.0	1.5	2.0
	$\overline{z}$	3.0	3.57	3.78	4.05	4.40

- $\psi \simeq 3.3$ for $d = 2$; $\psi \simeq 5.6$ for $d = 3$.

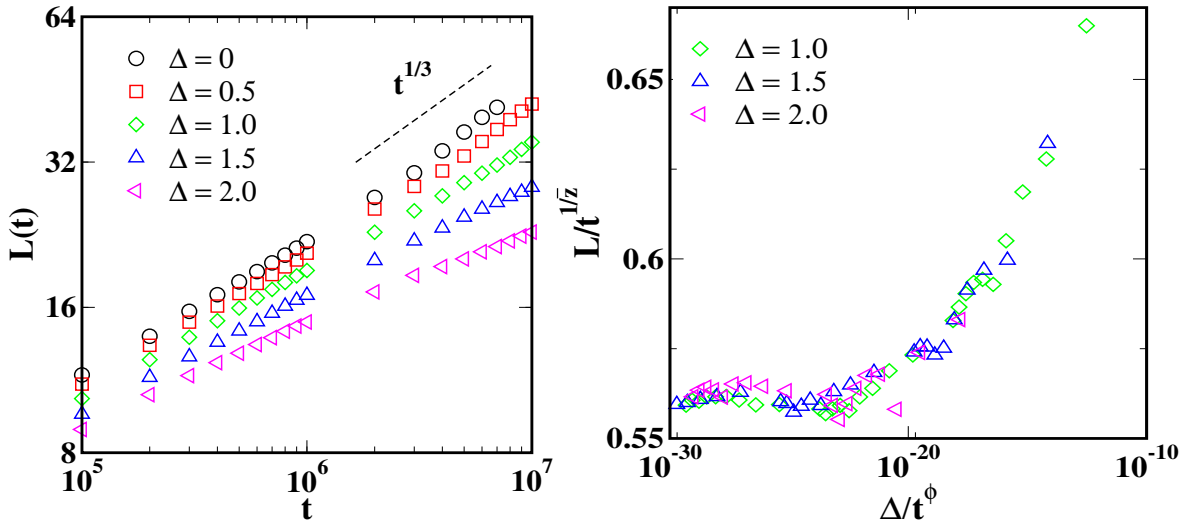

Kumar, VB, Puri, Europhys. Lett. 2017

Slow Logarithmic Growth and Rough Interfaces

- Domain growth in disordered systems proceeds via activation over barriers of energy $E_B \sim \epsilon_B L^{\psi}$. Here, ϵ_B is the barrier energy per unit length, and ψ is the barrier exponent.
- For curvature-driven growth in non-conserved systems,
  - $dL/dt = a(L,t)/L$.
- In systems with quenched disorder, **Lai, Mazenko, Valls, Phy. Rev. B 1988**
  - $a(L,t) = a_0 \exp(-\epsilon_B L^{\psi}/T)$,
  - $L(t) \sim (T\epsilon_B^{-1})^{1/\psi} (\ln t)^{1/\psi}$.
  - Same form from our scaling ansatz.
- Villain argued that the barrier exponent $\psi = 2 - \alpha$, where α is the *cusp exponent*. **(Villain, Phys. Rev. Lett., 1984)**

Fractal interfaces lead to slow logarithmic domain growth.

Summary

- Efficient algorithm to determine ground states ($T = 0$) of the RFIM in $d = 3$.
- Accurate estimation of the critical disorder strength Δ_c in isometric lattices; Identification of fractal interfaces; Accurate estimation of the fractal dimension d_f.
- Interfacial textures in para and ferro phase are distinct. In the para phase, the cusp exponent $\alpha \simeq 0.5$ is universal. In the ferro phase, it exhibits dependence on disorder and local environment.
- Comprehensive MC study of domain growth after a temperature quench ($T \neq 0$) in the RFIM with conserved dynamics in $d = 3$. (No knowledge of equilibrium states.)
- Observe *clean* cross-overs from a disorder-dependent power-law growth to a disorder-independent logarithmic growth.
- Fractal interfaces have important implications in growth, relaxation and response.

Scaling ansatz to determine $\bar{z}$ and ψ Corberi et al. PRE 2012, 2013

- $$L(t,\Delta) \sim t^{1/z_{\rm eff}} = t^{1/z} F(\Delta/t^{\phi}), \tag{3}$$

$$F(x) \sim \begin{cases} \text{const.}, & \text{for } x \to 0, \\ x^{1/\phi z}\ \ell\left(x^{-1/\phi}\right), & \text{for } x \to \infty. \end{cases} \tag{4}$$

  $z_{\rm eff}$ is the *effective* growth exponent, ϕ is the crossover exponent.

- The evaluation of $z_{\rm eff}$ is easier using the inverted form:

$$t = L^z G(L/\lambda). \tag{5}$$

  Here, $\lambda = \Delta^{1/\phi z}$ is the crossover length scale and $G(y) = [F(x)]^{-z}$.

- The effective exponent as a function of y $(= L/\lambda)$ is then

$$z_{\rm eff}(y) = \frac{\partial \ln t}{\partial \ln L} = z + \frac{\partial \ln G(y)}{\partial \ln y}. \tag{6}$$

Exponents $\bar{z}$, ϕ and ψ

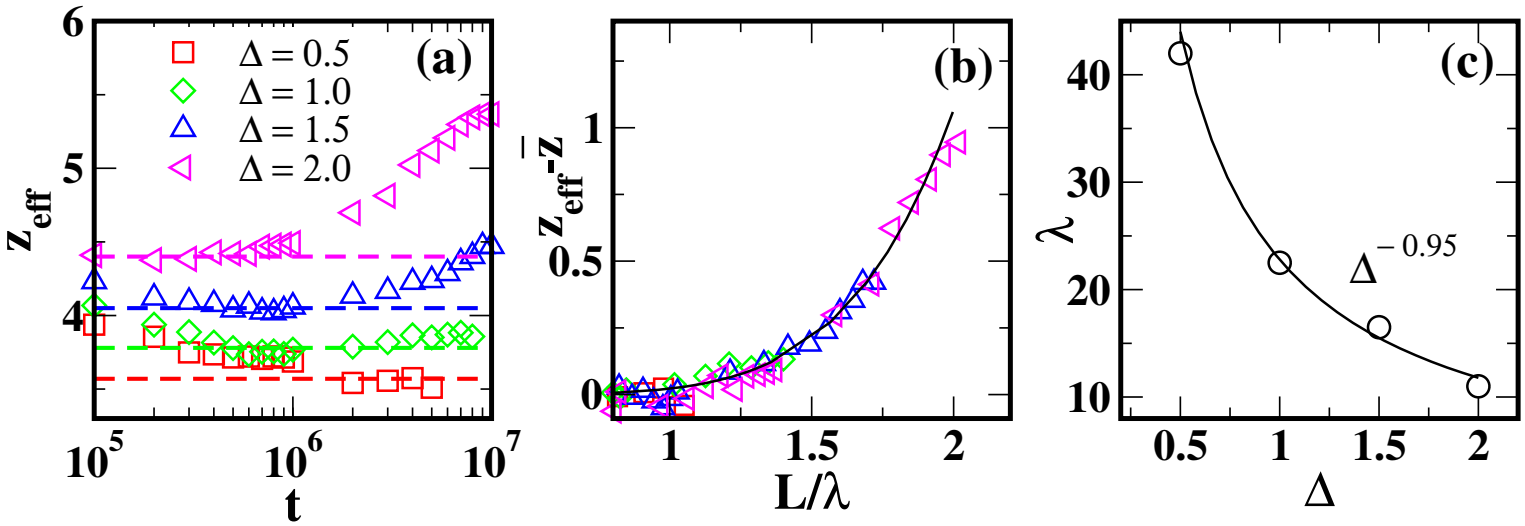

(a) $z_{\rm eff} = [d(\ln L)/d(\ln t)]^{-1}$ vs. t (semi-log).
Dashed lines: disorder-dependent exponents $\overline{z}(\Delta)$ of the power law.
This is followed by a late regime where $z_{\rm eff}$ is time-dependent.

(b) Scaling collapse of $z_{\rm eff} - \overline{z}$ vs. L/λ, where $\lambda = \Delta^{1/\phi\bar{z}}$. The solid line is the best power-law fit: $z_{\rm eff} - \overline{z} = b(L/\lambda)^{\psi}$ with $b \simeq 0.022$, $\psi \simeq 5.6$.

(c) Δ-dependence of λ. Power-law fit: $\lambda \sim \Delta^{-0.95}$.

Kumar, VB & Puri, EPL, 117, 10012, 2017

Exponents and data collapse

Δ	0	0.5	1.0	1.5	2.0
$\bar{z}$	3.0	3.57	3.78	4.05	4.40
$\lambda\ (=\Delta^{1/\phi\bar{z}})$	∞	42.1	22.5	16.5	11.0

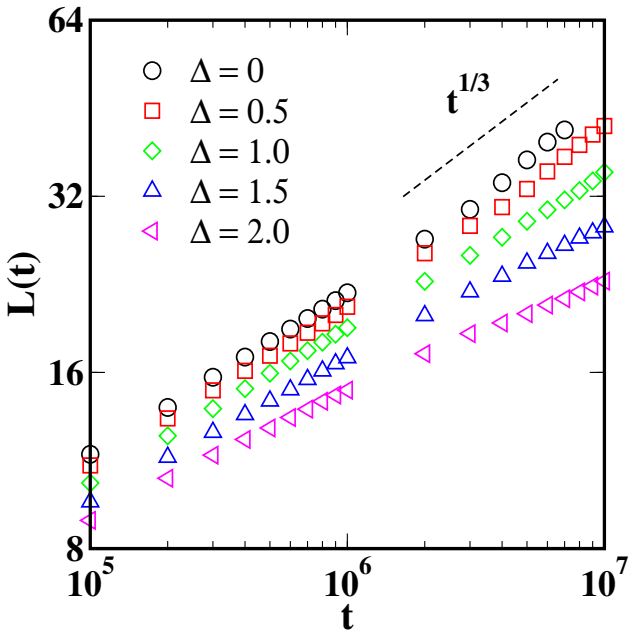

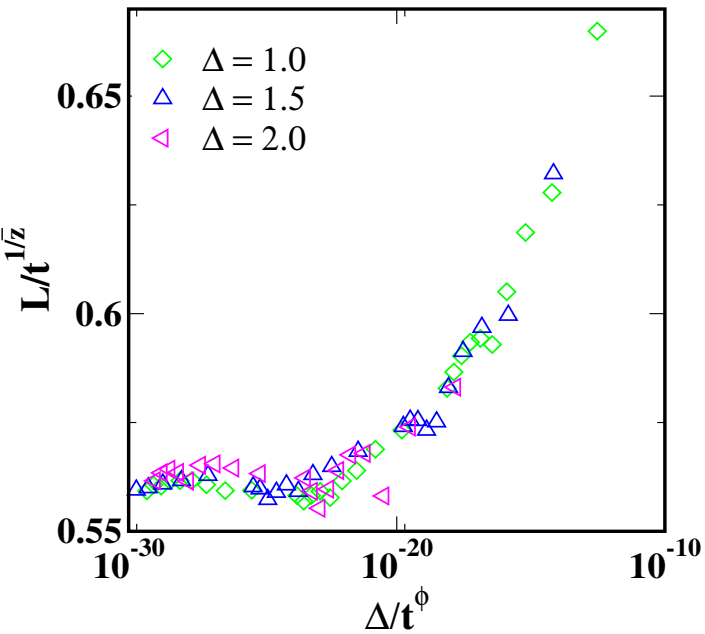

Kumar, VB & Puri, EPL, 117, 10012, 2017

Why logarithmic domain growth?

Generalizing Eqs. (1)-(4) by replacing $z \to \bar{z}$,

$$\frac{\partial \ln G(y)}{\partial \ln y} = z_{\rm eff} - \bar{z} = by^{\psi} \quad \Rightarrow \quad G(y) \sim \exp\left(\frac{b}{\varphi} y^{\psi}\right). \tag{7}$$

Substituting in Eq. (5) results in the asymptotic logarithmic growth form:

$$y = \frac{L}{\lambda} \simeq \left[\frac{\psi}{b} \ln(t/\lambda^{\bar{z}})\right]^{1/\psi}. \tag{8}$$

The disorder-independent exponent ψ has great physical significance:

- Domain growth in disordered systems (e.g. RFIM) proceeds via activation over barriers of energy $E_B \sim \epsilon_B L^{\psi}$,
  ϵ_B: barrier energy per unit length; ψ: barrier exponent.
- The asymptotic growth law is then logarithmic:
  $L(t) \sim (T/\epsilon_B)^{1/\psi} (\ln t)^{1/\psi}$.

Huse & Henley, PRL 1985; Lai et al., PRB 1988